Aspergillus nidulans biofilm formation modifies cellular architecture and enables light-activated autophagy

Dale E. Lingo[a], Nandini Shukla[a,b,†], Aysha H. Osmani[a], and Stephen A. Osmani[a,*]
[a]Department of Molecular Genetics and [b]The Ohio State Biochemistry Program, The Ohio State University, Columbus, OH 43210

ABSTRACT **After growing on surfaces, including those of medical and industrial importance, fungal biofilms self-generate internal microenvironments. We previously reported that gaseous microenvironments around founder *Aspergillus nidulans* cells change during biofilm formation causing microtubules to disassemble under control of the hypoxic transcription factor SrbA. Here we investigate if biofilm formation might also promote changes to structures involved in exocytosis and endocytosis. During biofilm formation, the endoplasmic reticulum (ER) remained intact but ER exit sites and the Golgi apparatus were modified as were endocytic actin patches. The biofilm-driven changes required the SrbA hypoxic transcription factor and could be triggered by nitric oxide, further implicating gaseous regulation of biofilm cellular architecture. By tracking green fluorescent protein (GFP)-Atg8 dynamics, biofilm founder cells were also observed to undergo autophagy. Most notably, biofilm cells that had undergone autophagy were triggered into further autophagy by spinning disk confocal light. Our findings indicate that fungal biofilm formation modifies the secretory and endocytic apparatus and show that biofilm cells can also undergo autophagy that is reactivated by light. The findings provide new insights into the changes occurring in fungal biofilm cell biology that potentially impact their unique characteristics, including antifungal drug resistance.**

Monitoring Editor
Howard Riezman
University of Geneva

Received: Nov 19, 2020
Revised: Mar 29, 2021
Accepted: Apr 1, 2021

INTRODUCTION

In nature, many cells exist within organs or colonies in a viable but static nongrowing state and generate their own unique microenvironments. The microenvironment of cells plays important roles in many biological processes including tumorigenesis (Wang *et al.*, 2017) and drug resistance of microbial pathogens. With regards to microbial infections, the physiological state of static cells impacts how pathogens respond to drug treatment. For example, fungal biofilm cells generate their own microenvironments and resistance to antifungal treatments (Desai *et al.*, 2014; Kaur and Singh, 2014; Kowalski *et al.*, 2020). On the more positive side, solid state fungal biofilms can be the preferred mode of growth in fungal driven fermentations, as well as production of enzymes, organic acids, and other bioactive compounds (Gutierrez-Correa *et al.*, 2012; Park *et al.*, 2017). However, the biological changes occurring within fungal biofilm cells which distinguish them from unattached planktonically growing cells is not well understood. There is therefore considerable interest in understanding how the physiology and cell biology of forming biofilm cells get modified (Gonzalez-Ramirez *et al.*, 2016) and how this might be leveraged to help remediate negative fungal biofilm characteristics, such as during food spoilage and infections. Similarly, further understanding of changes occurring within fungal biofilms could help enhance their industrial applications (Villena and Gutierrez-Correa, 2007).

Biofilm formation starts with the attachment of initiator cells to a surface (Ramage *et al.*, 2011; Gonzalez-Ramirez *et al.*, 2016). For *Aspergillus nidulans* biofilm formation, growth is initiated using asexual spores called conidia. Germinating conidia have a tenacious

This article was published online ahead of print in MBoC in Press (http://www.molbiolcell.org/cgi/doi/10.1091/mbc.E20-11-0734) on April 7, 2021.

†Present address: Section of Molecular Biology, Division of Biological Sciences, University of California, San Diego, La Jolla, CA 92093-0322.

*Address correspondence to: Stephen A. Osmani (osmani.2@osu.edu).

Abbreviations used: ER, endoplasmic reticulum ; ERESs, ER exit sites; GFP, green fluorescent protein; MT, microtubule; PAS, phagophore assembly site; ROS, reactive oxygen species.

capacity to attach to surfaces including glass. For example, during liquid growth in unsiliconized glass flasks, germinating conidia will attach and grow on the sides of conical flasks even when the flasks are rotated at a high speed. Growth on a surface as a biofilm is likely the preferred mode of growth for *A. nidulans* and many other Aspergillus species (Gravelat *et al.*, 2010). To track the cell biology of founder biofilm cells, they are grown in dishes containing a coverslip at their bottom. Germinating conidia attach and grow on the coverslip and can be observed during biofilm formation using an inverted spinning disk confocal microscope system (Shukla *et al.*, 2017). Founder tip cells initially avoid each other as they grow but then some stop growing, getting trapped at the base of the forming biofilm. During biofilm development, microtubules (MTs) then get depolymerized within the founder cells in a manner that was reversible by gaseous exchange above the culture dish (Shukla *et al.*, 2017). MT disassembly failed to occur in strains lacking the hypoxic transcription factor SrbA, indicating that changing gaseous microenvironments play a role in regulating biofilm cell biology. SrbA (Willger *et al.*, 2008; Bat-Ochir *et al.*, 2016) is the Aspergillus orthologue of the *Schizosaccharomyces pombe* sterol regulatory element-binding protein 1 (Sre1), a transcription factor (Hughes *et al.*, 2005) required for adaptation to hypoxia. As seen in other fungi, deletion of *srbA* in *A. nidulans* does not affect growth on agar plates under normoxia but inhibits growth under hypoxic growth conditions (Bat-Ochir *et al.*, 2016). Collectively the findings indicate that the cell biology of founder biofilm cells is modified in a process involving self-generated hypoxia caused by metabolic O_2 depletion outcompeting its rate of replacement via diffusion, and SrbA regulation (Shukla *et al.*, 2017).

In the current study, we aimed to ask if the cell biology of biofilm founder cells is changed beyond MT depolymerization and if other more widespread systemic changes in subcellular architecture might occur under control of SrbA. The primary function of cytoplasmic MTs is to transport membranous cargoes, including early endosomes and post-Golgi vesicles (Abenza *et al.*, 2009; Pantazopoulou *et al.*, 2014). Therefore, the impairment of cargo transport resulting from MT-depolymerization during biofilm formation could be coordinated with functional or structural changes in upstream and downstream steps of the membrane trafficking pathway. Furthermore, we reasoned that during biofilm formation the growth arrest of founder tip cells might be accompanied by blockages or flux-changes in secretion and endocytosis, two processes whose coordinated action accomplishes polarized tip growth (Riquelme *et al.*, 2018). To test these ideas, we first investigated the dynamics of the central components of the membrane trafficking pathway and found that while the peripheral endoplasmic reticulum (ER) remained intact, the transitional ER, the early and late Golgi cisternae, and endocytic actin patches were dramatically modified. Also, during these studies we discovered that autophagy, tracked by following green fluorescent protein (GFP)-Atg8 localization, was reactivated during spinning disk confocal imaging of biofilm founder cells and we discuss the potential molecular basis for this effect.

RESULTS

The ER remains intact during biofilm formation

To investigate if the protein secretory apparatus might change during biofilm formation, we first imaged the ER using Sec63-GFP, a marker previously used to monitor ER dynamics in *A. nidulans* (Markina-Inarrairaegui *et al.*, 2013). We also tracked EB1-mCherry comets which locate at the ends of growing MTs. EB1-mCherry undergoes dispersal from comets during early biofilm formation after MTs disassemble and so can be used as a marker for biofilm formation (Shukla *et al.*, 2017). Cells were imaged after 24 h of growth, representing an early stage of biofilm formation prior to MT disassembly and EB1-mCherry dispersal (Figure 1A, Day 1). Cells were additionally imaged after 3 d of growth by which time biofilm maturation had promoted MT disassembly and EB1-mCherry dispersal (Figure 1A, Day 3). As previously reported (Markina-Inarrairaegui *et al.*, 2013), Sec63-GFP locates throughout the ER including around nuclei at the outer nuclear envelope, as well as in cytoplasmic ER strands and tubules, many of which were plasma membrane associated (Figure 1A, Day 1). After biofilm formation, no obvious alterations in ER structures were observed with, or without, SrbA function (Figure 1, A and B).

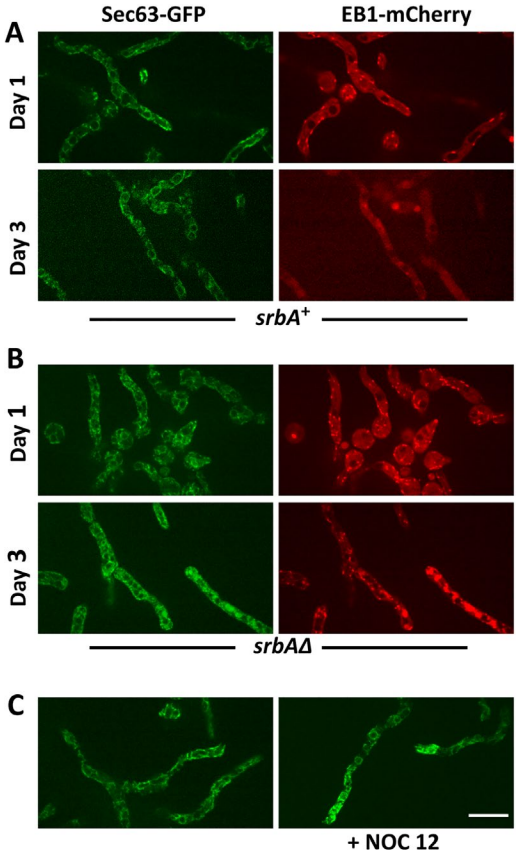

FIGURE 1: The ER appears unchanged during biofilm formation. (A) The ER marker Sec63-GFP and the MT +End-binding protein EB1-mCherry (strain SO1812) before (Day 1) and during biofilm formation (Day 3). EB1-mCherry undergoes dispersal from comets during biofilm formation but the Sec63-GFP ER pattern remained unchanged. (B) Same as for A but in a strain with *srbA* deleted (*srbA*Δ, strain SO1810). We observed some vacuolelike signal in the red channel of some *srbA*Δ cells which represents autofluorescence specific to *srbA*Δ cells; see Supplemental Figure S1. (C) The ER marker Sec63-GFP (strain SO1812) before and 15 min after treatment with the NO donor NOC-12 as indicated. Bar, 10 μm.

Without SrbA cells can accumulate autofluorescent species during biofilm formation

During biofilm formation of Δ*srbA* cells, in addition to EB1-mCherry comets, other red signals appeared in vacuolelike structures. These additional signals were absent from WT biofilm cells that were similarly tagged. To distinguish if the additional red signal in Δ*srbA* biofilm cells was from autofluorescence specific to Δ*srbA* cells, we imaged WT and Δ*srbA* cells during biofilm formation which lacked

fluorescent protein markers (Supplemental Figure S1). In wild-type cells, no red autofluorescence was apparent before or during biofilm formation. However, in Δ*srbA* cells, red autofluorescence became apparent during biofilm maturation (Supplemental Figure S1) within vacuolelike structures (Veses *et al.*, 2008). While autofluorescence can be a confounding issue during microscopy, it is possible to discern differences between autofluorescence and tagged EB1 because of their distinctive patterns and movements.

ER exit sites are modified in an SrbA-dependent manner during biofilm formation

We next investigated the behavior of ER exit sites (ERESs) during biofilm formation by visualizing the COPII coat component Sec23 (Rossanese *et al.*, 1999; Budnik and Stephens, 2009) C-terminally tagged with GFP. Sec23-GFP has previously been employed to track ERESs in *A. nidulans* (Pantazopoulou and Penalva, 2009) and shown to locate at many small foci with an increased density toward cell tips (Pantazopoulou and Penalva, 2009), a pattern we also observed (Figure 2A, Day1). During the initial growth phase of biofilm formation, the founder cells contained many ERES foci and EB1-mCherry located to comets (Figure 2A, Day 1). During biofilm formation, EB1-mCherry dispersed from comets and Sec23-GFP was observed to locate to fewer, larger foci (Figure 2A, Day 3).

To ask if the Sec23 ERES modifications were dependent on the hypoxic transcription factor SrbA, the experiment was repeated under the same biofilm forming conditions but in a Δ*srbA* strain lacking SrbA. Without SrbA function, EB1-mCherry remained at comets during biofilm formation as previously noted (Shukla *et al.*, 2017), and Sec23-GFP also remained unchanged, continuing to locate to numerous ERES foci (Figure 2B). This shows that, like MT disassembly, modification of ERESs during biofilm formation is dependent on SrbA.

Nitric oxide treatment phenocopied the effects of biofilm formation on ERES and EB1

Treatment of *A. nidulans* cells with hydrogen sulfide (H_2S) caused MT disassembly and dispersal of EB1 from comets, as occurs in biofilm cells (Shukla *et al.*, 2017). It was suggested these effects could be caused by H_2S inhibiting cytochrome *c* oxidase and respiration (Mustafa *et al.*, 2009). We therefore tested if nitric oxide (NO), which also inhibits cytochrome *c* oxidase, might have similar effects and cause the changes to ERESs as seen during biofilm formation. NOC-12 [N-Ethyl-2-(1-ethyl-2-hydroxy-2-nitrosohydrazino)ethanamine] is a NO donor with a half-life, at pH 7.4, of over 5 h. Notably, the ER pattern of Sec63-GFP was not modified during biofilm formation (Figure 1, A and B) nor did NO treatment notably modify ER structure of growing nonbiofilm cells (Figure 1C). In contrast, treatment of growing nonbiofilm cells with NOC-12 for 15 min caused the conversion of Sec23-GFP from small ERES foci to fewer larger foci (Figure 2C, +NOC-12), a transition mirroring what happens to ERES foci during biofilm formation (Figure 2A). We conclude that NO promotes similar effects on Sec23-GFP as occurs during biofilm formation.

The early Golgi marker GrhA is modified in an SrbA-dependent manner during biofilm formation and after NO treatment

The *A. nidulans* orthologue of *Saccharomyces cerevisiae* Grh1p (termed GrhA) endogenously C-terminally tagged with GFP acts as an early Golgi marker in *A. nidulans* (Pantazopoulou and Penalva, 2009). In yeast, Grh1p targets the coiled-coil tether Bug1 to the early Golgi and interacts with the COPII Sec23/24 subcomplex

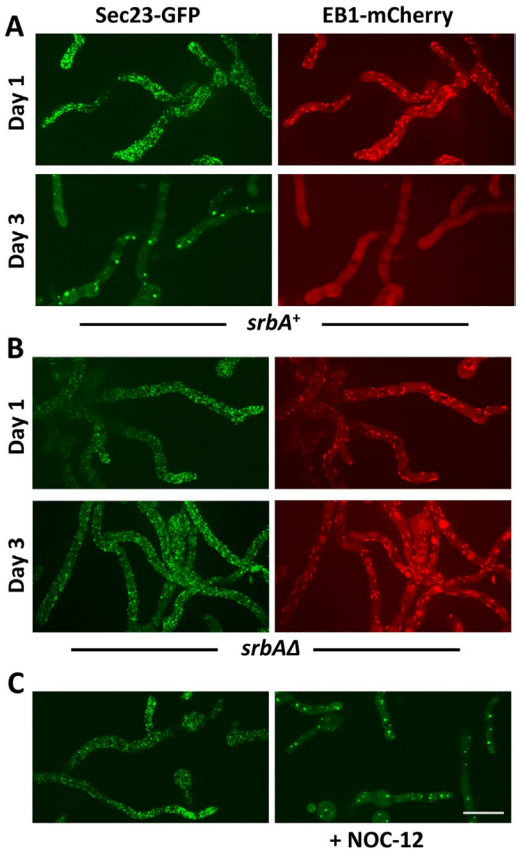

FIGURE 2: ERES are modified in an SrbA-dependent manner during biofilm formation and by NO treatment. (A) The ER exit site marker Sec23-GFP and the MT +End marker protein EB1-mCherry (strain SO1800) at Day 1, prior to biofilm formation and Day3, during biofilm formation. During biofilm formation EB1-mCherry disperses from comets and Sec23-GFP changes from locating at multiple small ER exit site structures to fewer, larger foci. (B) Same as for A in a strain in which *srbA* is deleted (*srbA*Δ, strain SO1799) when neither EB1-mCherry nor Sec23-GFP change during biofilm formation. (C) Images of Sec23-GFP (strain SO1800) before, and 15 min after, treatment with the NO donor NOC-12 as indicated. Bar, 10 μm.

(Behnia *et al.*, 2007). In nonbiofilm *A. nidulans* cells, GrhA-GFP locates to foci that are less abundant than those of the ERES marker Sec23-GFP (Pantazopoulou and Penalva, 2009) a pattern we also observed (Figure 3A, Day1). During biofilm formation GrhA relocates to fewer, larger foci (Figure 3A, Day 3) and, similar to Sec23, this transition was dependent on SrbA (Figure 3B). The transition of GrhA-GFP to fewer larger foci, as seen during biofilm formation, was recapitulated by NO treatment of growing nonbiofilm cells (Figure 3C).

Golgi organization is modified in an SrbA-dependent manner during biofilm formation and after NO treatment

A *trans*–Golgi-specific reporter construct termed *gpdA*mini::*mRFP-PH*OSBP, which expresses the pleckstrin homology domain of the human oxysterol binding protein (PH^{OSBP}) fused to mRFP, was developed as a Golgi marker in *A. nidulans* (Pantazopoulou and Penalva, 2009). As previously observed, mRFP-PH^{OSBP} locates in a tip-polarized pattern of foci representing *trans*-Golgi cisternae (Pantazopoulou and Penalva, 2009; Figure 4A, Day 1). Notably, the *trans*-Golgi was seen to undergo modifications during biofilm formation with mRFP-PH^{OSBP} then locating throughout the cytoplasm (Figure 4A,

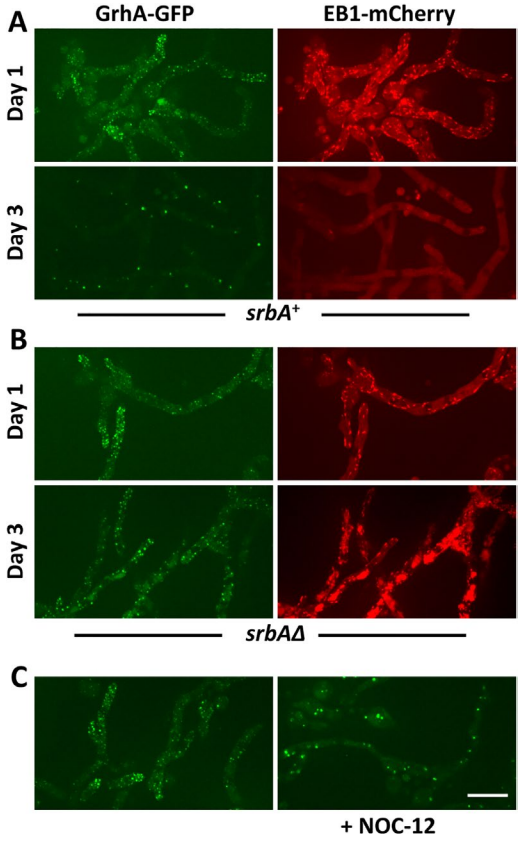

FIGURE 3: The early Golgi marker GrhA is modified in an SrbA-dependent manner during biofilm formation and by NO treatment. (A) The early Golgi marker protein GrhA-GFP and the MT +End marker protein EB1-mCherry (strain SO1804) at Day 1 prior to biofilm formation and during biofilm formation on Day 3. During biofilm formation (Day 3), EB1-mCherry disperses from comets and GrhA-GFP changes from locating at numerous early Golgi foci to fewer larger foci. (B) Same as for A but in a strain in which *srbA* is deleted (*srbA*Δ, strain SO1802) and neither EB1-mCherry nor GrhA-GFP change during biofilm formation. (C) The early Golgi marker protein GrhA-GFP (strain SO1804) before and 15 min after treatment with the NO donor NOC-12 as indicated. Bar,10 μm.

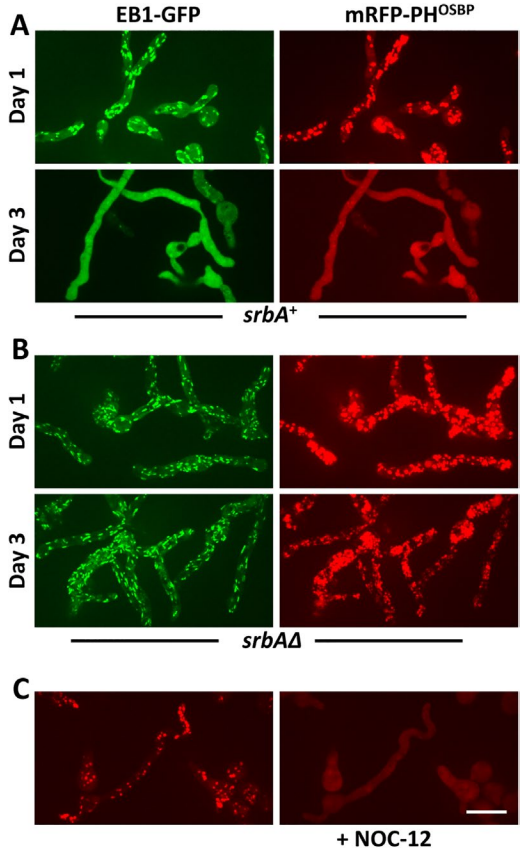

FIGURE 4: Golgi puncta are disassembled in an SrbA-dependent manner during biofilm formation and after NO treatment. (A) The *trans*–Golgi-specific reporter mRFP-PH^{OSBP} and the MT +End marker protein EB1-GFP (strain SO1819) prior to biofilm formation (Day 1) and during biofilm formation on Day 3. During biofilm formation (Day 3), EB1-GFP disperses from comets and the *trans*–Golgi-specific protein mRFP-PH^{OSBP} also disperses. (B) Same as for A but in a strain in which *srbA* is also deleted (*srbA*Δ, SO1821) and neither EB1-GFP nor mRFP-PH^{OSBP} change during biofilm formation. (C) The *trans*–Golgi-specific reporter mRFP-PH^{OSBP} (strain SO1819) before and 15 min after treatment with the NO donor NOC-12 as indicated. Bar, 10 μm.

Day 3). As expected, EB1 also dispersed from comets as biofilms formed (Figure 4A, Day 3). However, in the absence of SrbA, mRFP-PH^{OSBP} remained associated with Golgi and failed to disperse, and EB1 remained at comets (Figure 4B, Day 3). The diffusion of mRFP-PH^{OSBP} from Golgi was also triggered after treatment of growing nonbiofilm cells with NO (Figure 4C). Notably, it was previously observed that mounting cells under microscope coverslips caused mRFP-PH^{OSBP} to relocate from Golgi to the cytoplasm in general (Pantazopoulou and Penalva, 2009). It was proposed that either hypoxia or mechanical pressure might cause this effect and our data support the idea that hypoxia is more likely to be the cause for mRFP-PH^{OSBP} dispersal when cells are mounted under coverslips as previously observed (Pantazopoulou, 2016).

Endocytic internalization actin patches are modified in an SrbA-dependent manner during biofilm formation

Given that the protein secretory apparatus is modified during biofilm formation (Figures 1–4), we asked if endocytosis might also be affected. We explored how the orthologue of the endocytic actin patch marker Abp1 of *S. cerevisiae*, termed AbpA in *A. nidulans* (Araujo-Bazan *et al.*, 2008), might change during biofilm formation. Endogenously mRFP tagged AbpA locates to patches at the cell periphery as a marker for endocytic actin patches, with some patches forming a subapical cell tip ringlike pattern (Araujo-Bazan *et al.*, 2008; Figure 5A, Day 1). During biofilm development, AbpA-mRFP locations are modified such that larger, less abundant foci appear while the small peripheral patches were no longer apparent (Figure 5A, Day 3). Notably, it has been shown that treatment of cells to lower ATP using 10 mM sodium azide plus 10 mM sodium fluoride treatment also caused depolarization and clustering of AbpA patches into larger structures (Araujo-Bazan *et al.*, 2008). Most of the changes occurring to AbpA-mRFP during biofilm formation failed to occur in strains lacking SrbA function, although the tip-centric location of the peripheral foci appeared diminished (Figure 5B, Day 3).

Autophagy is activated during biofilm maturation

Autophagy enables cells to reutilize cytoplasmic constituents and those sequestered in organelles via their breakdown in vacuoles/lysosomes for recycling (Parzych and Klionsky, 2014; Delorme-Axford *et al.*, 2015). Autophagy in filamentous fungi can be triggered by

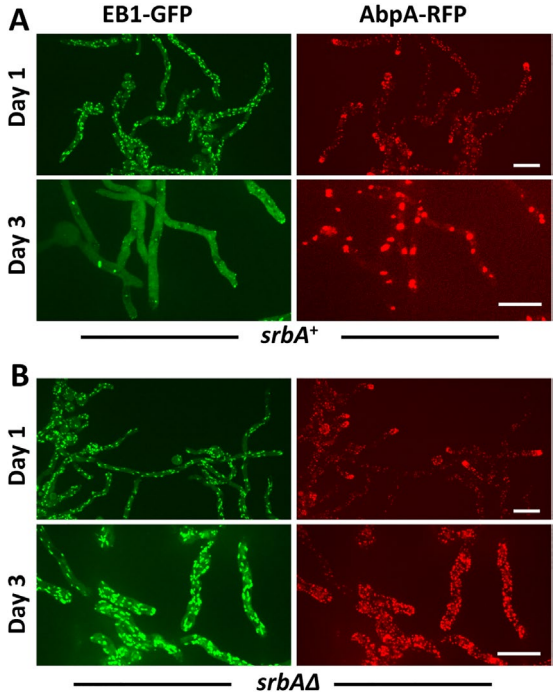

FIGURE 5: Endocytic internalization actin patches are modified in an SrbA-dependent manner during biofilm formation. (A) The endocytic actin patch marker AbpA-mRFP, and the MT +End protein EB1-GFP (strain SO1808) prior to biofilm formation (Day 1) and after biofilm formation (Day 3). (B) Same as for A but in a strain in which *srbA* is also deleted (*srbA*Δ, strain SO1806). In the absence of SrbA, EB1-GFP does not change during biofilm formation nor do AbpA-mRFP foci but they do display a less tip-centric distribution. Bar, 10 μm.

starvation and can also occur in older basal cells of hyphae within colonies (Pollack *et al.*, 2009; Voigt and Poggeler, 2013). We tracked GFP-Atg8, the *A. nidulans* orthologue of the yeast autophagy marker Atg8p (Klionsky *et al.*, 2003; Xie *et al.*, 2008), under conditions previously used to study nitrogen starvation-induced autophagy in *A. nidulans* (Pinar *et al.*, 2013). We recapitulated the studies of Pinar *et al.* 2013, who defined GFP-Atg8 locations after nitrogen starvation. Prior to nitrogen limitation, GFP-Atg8 locates throughout the cytoplasm as well as distinct foci (Figure 6A, Pre N starvation) that represent phagophore assembly sites (PAS) as previously reported (Pinar *et al.*, 2013). After nitrogen starvation, to trigger autophagy, GFP-Atg8 gets delivered into vacuoles and, because GFP is resistant to proteolysis, the GFP signal accumulates within vacuoles (Pinar *et al.*, 2013; Figure 6A, Post N starvation). The processing and accumulation of GFP-Atg8 within vacuoles after nitrogen starvation depend on other autophagy genes, including *atg1* (Pinar *et al.*, 2013). Therefore, in Atg1-deleted cells, GFP-Atg8 remains at PAS foci after nitrogen starvation (Figure 6B, *atg1*Δ) as autophagy cannot occur.

Some vacuoles in our study were extended and tubular in shape, as previously reported for filamentous fungal vacuoles (Hyde *et al.*, 2002). It has been suggested such pleomorphic vacuolar structures could play roles in nutrient recycling in filamentous fungi (Shoji *et al.*, 2006a).

We next investigated if autophagy occurs during biofilm formation. After 3 d of biofilm development, GFP-Atg8 signal appeared predominantly within vacuoles indicating autophagy had been activated (Figure 6C, GFP-Atg8, Day 3). We confirmed this relocation of GFP-Atg8 to vacuoles was the result of autophagy within biofilm cells using a strain lacking Atg1 function (*atg1*Δ). The GFP-Atg8 signal remained at PAS foci in biofilm cells lacking Atg1 (Figure 6D, GFP-Atg8 *atg1*Δ). The data reveal that Atg1-dependent autophagy can be activated during biofilm maturation without media exchange to impose nitrogen starvation.

Autophagy is required for biofilm maturation

To determine if autophagy might play a role during biofilm formation, we asked if normal biofilm maturation was dependent on autophagy. Mature biofilms were allowed to develop over 7 d in strains with and without *atg1* function and biofilm formation was measured using their dry weight. In the absence of autophagy caused by deletion of *atg1*, less than half the biomass of WT biofilms was able to be generated, indicating that autophagy is required for normal biofilm maturation (Figure 6E).

Autophagy is activated by spinning disk confocal imaging of biofilm cells

GFP-Atg8 locates to PAS foci and a general cytoplasmic signal in prebiofilm cells (Figures 6, A and C, and 7A, Growing cells, 0 Min image). This pattern does not change noticeably during live cell imaging at 20-s intervals for an hour (Figure 7A, Growing cells, 30 and 60 min). PAS foci maintained their overall intensity throughout the imaging period, as can be seen from the kymograph of a representative cell (Figure 7B). The overall cellular intensity of the GFP-Atg8 signal was additionally seen to slowly decrease slightly, presumably due to photo bleaching caused by the repeated imaging (Figure 7A, Growing cells graph).

Imaging of biofilm cells under identical conditions (at 20-s intervals for an hour) caused quite dramatic effects not observed in growing cells prior to biofilm formation. In biofilm cells, because autophagy had been triggered, GFP-Atg8 signal located to vacuoles (Figure 7A, Biofilm cells, 0 Min). The GFP-Atg8 signal was not stable during imaging with the level of GFP fluorescence diminishing rapidly to below 10% the original levels and remained lowered for the rest of the imaging period (Figure 7A, Biofilm cells, 30 and 60 min, Biofilm cells graph). Although the overall level of GFP fluorescence decreased, an increase in the number of PAS foci was also surprisingly observed during imaging (Supplemental Video S1). These new PAS foci were transient in nature, forming then diminishing during imaging. When autophagy is triggered by nitrogen starvation, some PAS GFP-Atg8 foci mature into cup-shaped phagophores which develop into circular autophagosomes and then dissipate (Pinar *et al.*, 2013). Identical PAS maturation events were observed during imaging of biofilm cells (Figure 8A and Supplemental Video S1). The GFP-Atg8 PAS maturation process triggered after nitrogen starvation can be seen as characteristic cone-shaped traces in kymographs (Pinar *et al.*, 2013) which were also observed during imaging of biofilm cells (Figure 7C). In the particular biofilm cell shown in the Figure 7C kymograph, five sequential cone-shaped trace GFP-Atg8 PAS maturation events are apparent during the 1-h imaging period. The data indicate that autophagy can be triggered in biofilm cells during imaging. Prior imaging of autophagy tracking maturation of GFP-Atg8 PAS to phagophores after nitrogen starvation was carried out using 5-s delay image capture (Pinar *et al.*, 2013). We therefore compared the response of GFP-Atg8 in biofilm cells when imaged either at 20-s intervals, as done in Figure 7, or at the shorter 5-s intervals. Notably, the response was similar under both protocols, although the photobleaching occurred more rapidly with the 5 s delays, as might be expected, and GFP-Atg8 PAS were still seen to mature into phagophores (Supplemental Figure S2).

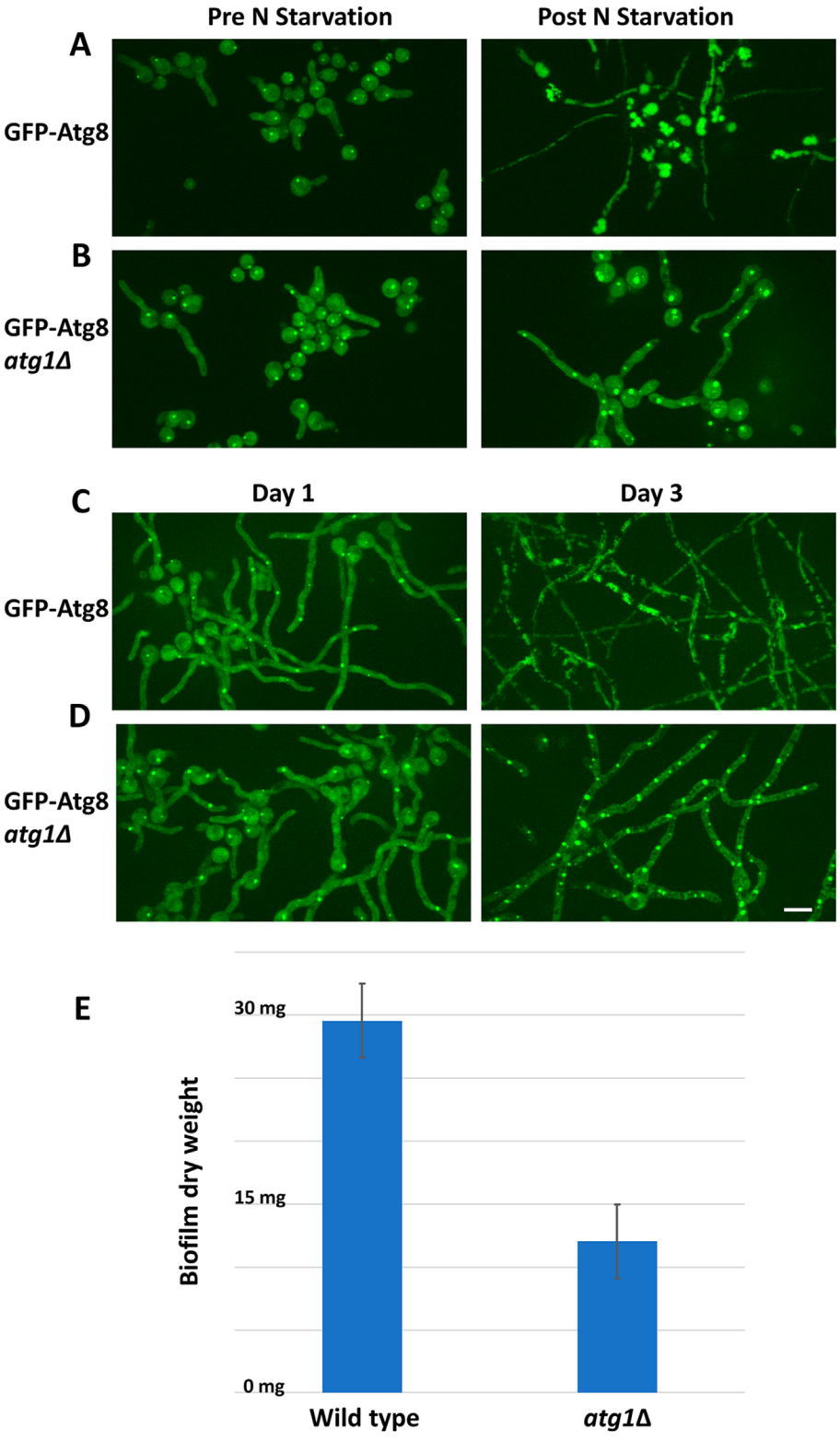

FIGURE 6: Autophagy can be activated during biofilm maturation. (A) Images of the autophagy marker GFP-Atg8 (strain MAD3474) before and after nitrogen starvation as indicated. (B) Same as for A but using a strain (MAD3476) lacking Atg1 (*atg1*Δ) which is required to trigger autophagy. GFP-Atg8 signal locates to vacuoles via autophagy after nitrogen starvation in an Atg1-dependent manner. (C) GFP-Atg8 during biofilm maturation changes from being at PAS foci in growing cells (Day 1) to being in vacuolelike structures during biofilm formation (Day 3). (D) Same as C but using a strain lacking Atg1 (*atg1*Δ) indicating the biofilm GFP-Atg8 changes reflect bonafide autophagy. (E) The biomass accumulated during biofilm formation with (wild type, strain MAD3474) and without Atg1 (*atg1*Δ, strain MAD3476) was measured as dry weight accumulated over 7 d growth. Bar, 10 μm.

We next investigated if the autophagy occurring during imaging of biofilm cells was triggered by the imaging light, or perhaps was something happening in cells throughout the imaging dish. We reasoned that if autophagy was triggered in response to imaging light it should not occur in adjacent unimaged cells. To investigate this, we repositioned the imaging dish after 1 h of imaging such that half the cells in the new field of view would be those previously imaged and half would not. In the previously imaged biofilm cells, GFP-Atg8 is located to PAS foci and phagophores, indicating autophagy had been triggered in the imaged cells. However, in the adjacent unimaged cells, all around those imaged, the GFP signal remains within vacuoles, indicating additional autophagy had not been triggered in them (Figure 8B). These observations indicate that, in biofilm cells expressing GFP-Atg8, autophagy is activated in response to the spinning disk confocal imaging light. To confirm the signals detected during light-activated autophagy in biofilm cells were dependent on GFP-Atg8, biofilm cells lacking any tagged protein were imaged in an identical manner. No signal was detected (Supplemental Figure S3). Finally, we tested if light-activated biofilm autophagy was dependent on Atg1 using a strain with *atg1* deleted and did not observe any GFP-Atg8 modifications past PAS foci (Supplemental Figure S2, A, D, and E).

DISCUSSION

Our findings show that during fungal biofilm formation, the ER remains largely unchanged when tracking Sec63-GFP, an integral membrane ER protein. Sec63 is a component of the ER translocon complexes that mediate the delivery of proteins synthesized in the cytosol into the ER lumen. The ER structure is sensitive to stress and Sec63-GFP in *A. nidulans* collapses and aggregates during artificially induced ER stress (Markina-Inarrairaegui *et al.*, 2013). The integrity of the ER within biofilm cells therefore indicates there is likely no general ER stress occurring within biofilm cells.

Subcellular modifications during biofilm development

While the ER appears apparently unmodified during biofilm maturation, subcellular changes do occur beyond the previously defined MT disassembly (Shukla *et al.*, 2017), including modification of ERES, the Golgi, as well as the sites of endocytosis. Using fluorescently tagged marker proteins that locate to these structures, each was found to be dramatically modified in the

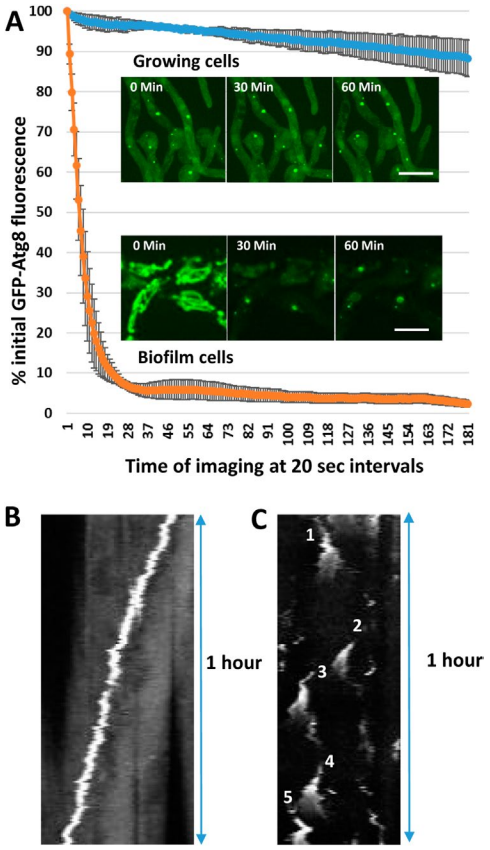

FIGURE 7: Autophagy is activated during spinning disk confocal imaging of biofilm founder cells expressing GFP-Atg8. (A) Graph plotting the levels of GFP fluorescence in growing nonbiofilm cells from GFP-Atg8 (strain MAD3474) during imaging at 20-s intervals over 1 h (blue line) and in similarly imaged biofilm cells (orange line). Error bars are SEM and $n = 3$. Inserted are images of representative cells at the start, middle, and end of imaging as indicated. (B) Kymograph showing GFP-Atg8 at a PAS in a growing nonbiofilm cell imaged at 20-s intervals for 1 h. (C) Kymograph showing GFP-Atg8 in a biofilm cell imaged at 20-s intervals for 1 h. Five examples of PAS formation and maturation into phagophores then autophagosomes, which dissipate, are numbered which display characteristic cone-shaped traces in kymographs during autophagy (Pinar *et al.*, 2013). Bar, 5 μm.

founder cells during biofilm formation. One explanation for why biofilm changes to Sec23-GFP, GrhA-GFP, mRFP-PH^{OSBP}, and AbpA-mRFP occur could be that they are a secondary effect of the MT depolymerization that happens as biofilms form. However, none of these markers are modified after MT depolymerization using the MT poison benomyl (Araujo-Bazan *et al.*, 2008; Pantazopoulou and Penalva, 2009), indicating their modifications are not a secondary effect of biofilm MT depolymerization.

The dramatic nature of the structural changes occurring to ERESs, the Golgi, and sites of endocytosis suggests that as biofilms mature, exocytosis and endocytosis likely become nonfunctional. For example, prior studies have shown that when traffic from the ER is impaired using a temperature-sensitive allele of SarA (the orthologue of yeast SAR1 ARF family GTPase required for transport vesicle formation during ER to Golgi protein transport), the ERES marker Sec23-GFP locates to large foci (Hernandez-Gonzalez *et al.*, 2018) in a manner very similar to what we have observed during biofilm formation and after NO treatment. Similarly, conditional impairment of ER traffic to the Golgi leads to Golgi disorganization, and PH^{OSBP} becomes delocalized to locate throughout the cytoplasm, again an effect we report during biofilm formation and after NO treatment. In terms of endocytosis, because the endocytic collar of actin patches is disrupted during biofilm formation, it is also likely that the recycling pathway that delivers endocytic membrane and cargo to the Golgi (Hernandez-Gonzalez *et al.*, 2018) also becomes nonfunctional. As we have previously documented that founder biofilm tip cells at the base of the biofilm stop growing, it is likely these cells have a limited requirement for exocytosis and endocytosis leading to their suppression as biofilms form. Regulation of the processes leading to changes in intracellular trafficking during biofilm formation is shown to involve gene regulation mediated by the hypoxic transcription factor SrbA. The pathways SrbA controls are known to be expansive and diverse, and SrbA is involved in fungal virulence and azole drug resistance (Willger *et al.*, 2008; Blatzer *et al.*, 2011; Chung *et al.*, 2014; Gsaller *et al.*, 2016). Our findings regarding the cell biology of biofilm cells that are dependent on SrbA therefore might provide clues to how SrbA is required for virulence and azole drug resistance.

Like MT disassembly, the ERES and the Golgi changes observed during biofilm formation could be recapitulated in growing nonbiofilm cells using NO. We had previously shown that H_2S was able to cause rapid MT disassembly in growing cells. Both H_2S and NO inhibit cytochrome *c* oxidase causing decrease in ATP production after mitochondrial respiration is impaired. This suggests that lowered ATP production could be the mechanism by which MTs, ERESs, and the Golgi get disassembled if cytochrome *c* oxidase becomes inhibited within forming biofilm cells. The findings also indicate that in the absence of SrbA, respiration might not get inhibited during biofilm formation, such that the normal subcellular changes seen during biofilm formation fail to occur.

ATP reduction has previously been shown to reversibly modify Golgi structure in human cells (Ranftler *et al.*, 2017). Energy depletion has also been well documented to cause major changes in yeast cells including reorganization of the cytoplasm and metabolic enzyme polymerization (Petrovska *et al.*, 2014; Marini *et al.*, 2020), a fluid to a solidlike state transition with cell shrinkage (Joyner *et al.*, 2016; Munder *et al.*, 2016), as well as phase separation events (Yoo *et al.*, 2019). It would be informative in future studies to investigate if such modifications occur in response to changing gaseous microenvironments within fungal biofilms.

Autophagy during biofilm development

It is typical to starve cells and/or treat them with rapamycin to initiate autophagy, as previously done in studies of autophagy in *A. nidulans* (Pinar *et al.*, 2013). However, our current study shows *A. nidulans* cells can trigger autophagy as biofilms form under growth conditions used to study fungal autophagy. Biofilm autophagy is dependent on the Atg1 protein kinase, indicating it represents activation of a normal autophagy pathway(s). We show autophagy is required for normal biofilm maturation as there is a reduction in biofilm biomass accumulation when *atg1* is deleted, revealing there is a functional role for activation of autophagy during biofilm maturation. In another Aspergillus species, *Aspergillus oryzae*, deletion of *atg1* prevents autophagy and causes defects in aerial hyphal growth, conidiation, and sclerotial formation (Yanagisawa *et al.*, 2013). It has also been shown in *A. oryzae* that autophagy is triggered in older basal cells of colonies which degrade peroxisomes, mitochondria, and nuclei within their vacuoles (Shoji *et al.*, 2010). This study also revealed a role for autophagy in colony growth and expansion under nutrient-limited growth conditions (Shoji *et al.*, 2006b) a similar situation also

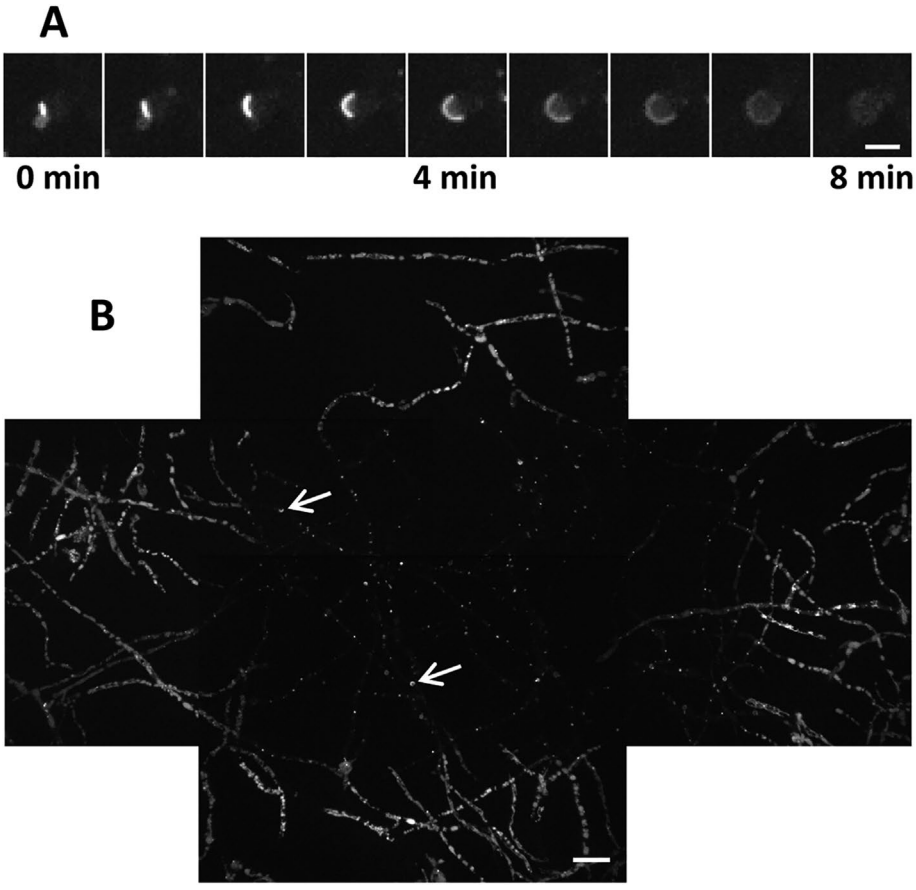

FIGURE 8: Autophagy is activated by imaging confocal spinning disk light in founder biofilm cells. (A) A time course of the dynamics of GFP-Atg8 (strain MAD3474) in biofilm cells during light-induced autophagy showing maturation of a PAS into a phagophore. Bar, 1 μm. (B) After imaging of GFP-Atg8 in biofilm cells that had undergone autophagy, additional images were collected around the initially imaged cells. The images were then manually aligned showing that the originally imaged cells have undergone autophagy with GFP-Atg8 at PAS and maturing phagosomes, (two examples are arrowed) while the previously unimaged cells have GFP-Atg8 still in vacuoles. The fact that only previously imaged biofilm cells, and not the surrounding cells, reactivated autophagy indicates it is the imaging illumination that causes activation of autophagy in biofilm cells in which autophagy had already occurred. Bar, 10 μm.

observed in *Aspergillus fumigatus* (Richie and Askew, 2008). Autophagy within the Aspergilli therefore seems to play roles during differentiation, colony growth and biofilm formation with these roles being more prominent in nutrient-poor conditions, including limited metal ions (Richie *et al*., 2007; Richie and Askew, 2008).

Further studies will be required to see what autophagy activation pathway(s) lead to biofilm-regulated autophagy (Corona Velazquez and Jackson, 2018), beyond the involvement of Atg1, and to better understand what mode(s) of autophagy are activated (Galluzzi *et al*., 2017). Given that hypoxia is generated within fungal biofilms and that hypoxia is a known trigger for autophagy (Mazure and Pouyssegur, 2010; Blagosklonny, 2013; Tan *et al*., 2016), it is possible that it is self-generated hypoxia that promotes biofilm autophagy.

Nutrient resources recycled within the older founder biofilm cells via autophagy could be made available to support growth or other processes, such as extracellular matrix formation, toward the biofilm surface. Based on proteomics, it has been suggested that selective ribosome autophagy might occur in *Candida orthopsilosis* biofilms (Pires *et al*., 2016), but our study might be the first to directly demonstrate activation of autophagy within a fungal biofilm. In addition, autophagy has been shown to be activated within filamentous fungal plant pathogens as they encounter nutrient-poor conditions during the infection process (Kershaw and Talbot, 2009; Zhu *et al*., 2019) and autophagy is required for fungal plant pathogenesis (Zhu *et al*., 2019). It will be interesting to investigate what microenvironmental changes might be responsible for activation of biofilm autophagy (Corona Velazquez and Jackson, 2018) but, as discussed further below, it is possible that reactive oxygen species (ROS) could be involved.

Biofilm autophagy is reactivated by light

Perhaps the most unexpected finding of this study is that spinning disk confocal light appears to activate autophagy in founder biofilm cells after they have already undergone autophagy. This is an intriguing finding. There is considerable interest in the photobiology of fungi (Idnurm *et al*., 2010; Idnurm, 2013; Corrochano, 2019) which perceive and respond to light to regulate many cellular processes including circadian rhythms, developmental processes, and stress responses (Corrochano, 2019). Several types of light receptor proteins have been identified in fungi including opsins, phytochromes, and cryptochromes (Yu and Fischer, 2019) and it remains to be determined if such proteins play a role in light-activated biofilm autophagy. However, another potential photoreceptor in our experiments, GFP, might also play a role.

Fluorescent proteins, including GFP species, have the capacity to generate ROS when illuminated and can act as genetically encoded photosensitizers to produce singlet oxygen and superoxide on illumination (Trewin *et al*., 2018). This feature is utilized in chromophore-assisted laser inactivation (Jacobson *et al*., 2008; Jarvela and Linstedt, 2014; Sano *et al*., 2014; Wojtovich and Foster, 2014) and has led to the design of fluorescent proteins with higher yield of ROS such as KillerRed (Bulina *et al*., 2006) and SuperNova (Takemoto *et al*., 2013). It is therefore possible that GFP in our experiments produces ROS during imaging illumination, particularly within biofilm cells. This would be consistent with the rapid reduction in GFP fluorescence during imaging of biofilm cells being the result of ROS-mediated photo bleaching (Greenbaum *et al*., 2000). Notably, the GFP signal within growing nonbiofilm cells is not sensitive to bleaching during imaging. ROS has previously been implicated as a trigger for autophagy (Azad *et al*., 2009; Scherz-Shouval and Elazar, 2011) with ROS potentially acting as signaling molecules (Scherz-Shouval *et al*., 2007). Alternatively, ROS-mediated protein and lipid damage might generate suitable substrate targets for autophagy leading to its activation.

There is precedent for light-activated ROS via GFP-like proteins being able to trigger autophagy. For example, targeting light-activated ROS generators to mitochondria promotes activation of mitophagy (Yang and Yang, 2011; Wang *et al*., 2012). Also,

Strain	Genotype[a]	Source
SO1681	*srbA*Δ::*pyrG*^{af}; EB1-mCh:: *pyro*A; *paba*A1; Δ*nku*A::*arg*B; *w*A3	This study
MAD2173	*pyrG*89; Δ*nku*A::*arg*B; *arg*B2; *pyro*A4; *sec63*-GFP::*pyrG*^{af}	(Markina-Inarrairaegui *et al.*, 2013)
SO1812	EB1-mCh::*pyroA*^{af}; *sec63*-GFP::*pyrG*^{af}; *y*A2	This study
SO1810	EB1-mCh::*pyroA*^{af}; *sec63*-GFP::*pyrG*^{af}; *srbA*Δ::*pyrG*^{af};*w*A3	This study
MAD2566	*pyrG*89; *nku*AΔ::bar; *pyro*A4; *sec23*-GFP::*pyrG*^{af}	(Pantazopoulou and Penalva, 2009)
SO1800	EB1-mCh::*pyroA*^{af}; *sec23*-GFP::*pyrG*^{af}; *w*A3	This study
SO1799	EB1-mCh::*pyroA*^{af}; *sec23*-GFP::*pyrG*^{af}; *srbA*Δ:: *pyrG*^{af}; wA3	This study
MAD2637	*pyrG*89; *nku*AΔ::bar; *pyro*A4; *grh*A-GFP::*pyrG*^{af}	(Pantazopoulou and Penalva, 2009)
SO1804	EB1-mCh::*pyroA*^{af}; *grh*A-GFP::*pyrG*^{af}; wA3	This study
SO1802	EB1-mCh::*pyroA*^{af}; *grh*A-GFP::*pyrG*^{af}; *srbA*Δ::*pyrG*^{af}; wA3	This study
NS420	*srbA*Δ::pyrG^{af}; EB1-GFP::*pyroA*^{af}; *pyrG89*; *pyroA4*; *pabaA1*;Δ*nkuA*::*argB*; *argB2*; *fwA1*; *chaA1*; *wa3*; *sE15*; *nirA14*	This study
MAD2243	wA4; *arg*B2; *pyro*A4[*pyro*A*-*gpdA*^{mini}::mRFP::PH^{osbp}]; (*niiA4*?)	(Pantazopoulou and Penalva, 2009)
SO1819	EB1-GFP::*pyroA*^{af}; *pyro*A4(*pyro*A*-gpdA^{mini}::mRFP::PH^{osbp}); wA3	This study
SO1821	EB1-GFP::*pyroA*^{af}; *pyro*A4(*pyro*A*-gpdA^{mini}::mRFP::PH^{osbp}); *srbA*Δ::*pyrG*^{af}; wA3	This study
SO1531	EB1-GFP:: *pyroA*^{af}; *srbA*Δ::*pyrG*^{af}; *arg*B2; wA3	This study
MAD1399	*paba*A1; *pyrG*89; *y*A2; *abp*A::mRFP::*pyrG*^{fum}	(Araujo-Bazan *et al.*, 2008)
SO1808	EB1-GFP::*pyroA*^{af}; *abpA*-mRFP::*pyrG*^{af}; wA3	This study
SO1806	EB1-GFP::*pyroA*^{af}; *abpA*-mRFP::*pyrG*^{af}; *srbA*Δ::*pyrG*^{af}; yA2	This study
MAD3474	*y*A2; *pyroA*4[*pyroA**-gdp^{mini}::GFP::*atg*8]; *pantoB*100	(Pinar *et al.*, 2013)
MAD3476	*pyroA*4[*pyro*A*-gdp^{mini}::GFP::*atg8*]; *atg1*Δ::*pyrG*^{Af}	(Pinar *et al.*, 2013)
SO1675	*srbA*Δ::*pyrG*^{af};*pyroA*4; wA3	This study
CDS746	wA3	(Suresh *et al.*, 2017)
SO1954	*y*A2; *pyroA*4[*pyroA**-gdp^{mini}::GFP::*atg*8]	This study
SO1840	*tom20*-mRFP::*pyrG*^{af} (*pyrG*89); *pyroA*4; *paba*A1	This study

[a]All strains carry *ve*A1.

TABLE 1: Strains used in this study.

nonmitochondrial-generated ROS can lead to activation of autophagy (Hoffmann *et al.*, 2019) and ROS generated in lysosomes promotes their autophagic turnover in a process termed lysophagy (Hung *et al.*, 2013).

Another mechanism by which light might cause reactivation of autophagy is through effects on the cellular energetic balance within founder biofilm cells. After biofilm autophagy has occurred, cells might reach a metabolic state incompatible with further autophagy. For example, because autophagy is an energy-dependent process, a limited capacity to generate sufficient ATP could hinder autophagy (Schellens *et al.*, 1988; Singh and Cuervo, 2011). If this was the case, the mechanism by which light reactivates autophagy could be by promoting increased ATP levels. This could involve NO, which is known to inhibit cytochrome *c* oxidase in a manner that is reversible by light (Lane, 2006; Hamblin, 2018; Osipov *et al.*, 2018).

CONCLUSIONS

Not many studies of fungal biofilm biology have addressed what happens to cellular architecture as biofilms develop. Our study reveals that as biofilms form and mature, the founder cells modify their cytoskeleton and the apparatus for exocytosis and endocytosis in a manner that requires the hypoxic transcription factor SrbA. Many genes have been shown to be regulated by SrbA to enable cells to survive hypoxia and our results suggest part of the SrbA-regulated response is to enable cells to enter a more dormantlike state. We speculate that part of the reason cells lacking SrbA cannot survive hypoxia is their inability to down-regulate the cellular processes needed to enter a less active state. Autophagy is also shown to be a modifier of cellular structure within biofilm cells and we find imaging light is able to trigger biofilm autophagy, potentially via illuminated GFP generation of ROS. There is great interest in light therapies and their mode of action (Serrage *et al.*, 2019) and our study, in a more general sense, provides additional evidence suggesting that light-activated autophagy (Kessel and Oleinick, 2009; Duan *et al.*, 2018) should be considered as a potential contributing factor in such treatment modalities.

MATERIALS AND METHODS

Request a protocol through *Bio-protocol*.

General techniques

Classical genetics, strain construction, media preparation, culture, and transformation of *A. nidulans* were carried out as described previously (Pontecorvo *et al.*, 1953; Yang *et al.*, 2004; Nayak *et al.*, 2006; Shukla *et al.*, 2017). Strains used in the study, genotypes, and source are listed in Table 1.

Biofilm formation and microscopy

Biofilm cultures were generated and tracked microscopically as described previously (Shukla *et al.*, 2017). For autophagy experiments, the nitrogen source and concentration were as used previously to study autophagy in *A. nidulans* (Pinar *et al.*, 2013). We did not add rapamycin during nitrogen starvation. For biofilm formation, conidia were inoculated at 2.5×10^5/ml in 3 ml minimal media in glass coverslip- bottomed dishes (MatTek, Ashland, MA), grown at room temperature over a 3-d period, and imaged each day such that prebiofilm and maturing biofilm cells were imaged. To measure biofilm maturation, biomass accumulated over 7 d of growth was determined as the dry weight of cells after desiccating for at least 3 d in a 50°C drying oven after media removal by blotting between paper towels. Spinning disk confocal systems (UltraVIEW ERS and UltraVIEW Vox CSUX1; PerkinElmer) were used as described previously (Shukla *et al.*, 2017; Suresh *et al.*, 2017). Images are presented as maximum intensity projections except those in Figure 1, which are single z images. ImageJ (National Institutes of Health) software was used to quantitate GFP levels by using Threshold settings to limit measured pixels to within cells, and measurements were taken using the Analyze Particles command. Values were then normalized as a percentage of total signal present in the first imaged cells.

NO treatment

NOC-12 was used from a stock 100 mM solution, made in 10 mM NaOH, to yield final concentrations between 50 and 100 μM to generate NO. The addition of the maximum levels of 10 mM NaOH used (30 μl in 3 ml) did not affect the pH of the buffered media and did not affect any of the proteins monitored. For the NO experiments, early stage prebiofilm cultures were used with NOC-12 being added and mixed into the culture media prior to imaging.

ACKNOWLEDGMENTS

We give a very heartfelt thank you to Miguel Peñalva for providing numerous strains used in the study and for his always very generous and insightful feedback, comments, and ideas. We also thank past and present members of the Osmani lab for their insights and support.

REFERENCES

Abenza JF, Pantazopoulou A, Rodriguez JM, Galindo A, Penalva MA (2009). Long-distance movement of Aspergillus nidulans early endosomes on microtubule tracks. Traffic 10, 57–75.

Araujo-Bazan L, Penalva MA, Espeso EA (2008). Preferential localization of the endocytic internalization machinery to hyphal tips underlies polarization of the actin cytoskeleton in Aspergillus nidulans. Mol Microbiol 67, 891–905.

Azad MB, Chen Y, Gibson SB (2009). Regulation of autophagy by reactive oxygen species (ROS): implications for cancer progression and treatment. Antioxid Redox Signal 11, 777–790.

Bat-Ochir C, Kwak JY, Koh SK, Jeon MH, Chung D, Lee YW, Chae SK. (2016). The signal peptide peptidase SppA is involved in sterol regulatory element-binding protein cleavage and hypoxia adaptation in Aspergillus nidulans. Mol Microbiol 100, 635–655.

Behnia R, Barr FA, Flanagan JJ, Barlowe C, Munro S (2007). The yeast orthologue of GRASP65 forms a complex with a coiled-coil protein that contributes to ER to Golgi traffic. J Cell Biol 176, 255–261.

Blagosklonny MV (2013). Hypoxia, MTOR and autophagy: converging on senescence or quiescence. Autophagy 9, 260–262.

Blatzer M, Barker BM, Willger SD, Beckmann N, Blosser SJ, Cornish EJ, Mazurie A, Grahl N, Haas H, Cramer RA (2011). SREBP coordinates iron and ergosterol homeostasis to mediate triazole drug and hypoxia responses in the human fungal pathogen Aspergillus fumigatus. Plos Genet 7, e1002374.

Budnik A, Stephens DJ (2009). ER exit sites–localization and control of COPII vesicle formation. Febs Lett 583, 3796–3803.

Bulina ME, Chudakov DM, Britanova OV, Yanushevich YG, Staroverov DB, Chepurnykh TV, Merzlyak EM, Shkrob MA, Lukyanov S, Lukyanov KA (2006). A genetically encoded photosensitizer. Nat Biotechnol 24, 95–99.

Chung D, Barker BM, Carey CC, Merriman B, Werner ER, Lechner BE, Dhingra S, Cheng C, Xu W, Blosser SJ, *et al.* (2014). ChIP-seq and in vivo transcriptome analyses of the Aspergillus fumigatus SREBP SrbA reveals a new regulator of the fungal hypoxia response and virulence. PLoS Pathog 10, e1004487.

Corona Velazquez AF, Jackson WT. (2018). So many roads: the multifaceted regulation of autophagy induction. Mol Cell Biol 38, e00303-18.

Corrochano LM (2019). Light in the Fungal World: From Photoreception to Gene Transcription and Beyond. Annu Rev Genet 53, 149–170.

Delorme-Axford E, Guimaraes RS, Reggiori F, Klionsky DJ (2015). The yeast Saccharomyces cerevisiae: an overview of methods to study autophagy progression. Methods 75, 3–12.

Desai JV, Mitchell AP, Andes DR (2014). Fungal biofilms, drug resistance, and recurrent infection. Cold Spring Harb Perspect Med 4, a019729.

Duan X, Chen B, Cui Y, Zhou L, Wu C, Yang Z, Wen Y, Miao X, Li Q, Xiong L, He J (2018). Ready player one? Autophagy shapes resistance to photodynamic therapy in cancers. Apoptosis 23, 587–606.

Galluzzi L, Baehrecke EH, Ballabio A, Boya P, Bravo-San Pedro JM, Cecconi F, Choi AM, Chu CT, Codogno P, Colombo MI, *et al.* (2017). Molecular definitions of autophagy and related processes. EMBO J 36, 1811–1836.

Gonzalez-Ramirez AI, Ramirez-Granillo A, Medina-Canales MG, Rodriguez-Tovar AV, Martinez-Rivera MA (2016). Analysis and description of the stages of Aspergillus fumigatus biofilm formation using scanning electron microscopy. BMC Microbiol 16, 243.

Gravelat FN, Ejzykowicz DE, Chiang LY, Chabot JC, Urb M, Macdonald KD, al-Bader N, Filler SG, Sheppard DC (2010). Aspergillus fumigatus MedA governs adherence, host cell interactions and virulence. Cell Microbiol 12, 473–488.

Greenbaum L, Rothmann C, Lavie R, Malik Z (2000). Green fluorescent protein photobleaching: a model for protein damage by endogenous and exogenous singlet oxygen. Biol Chem 381, 1251–1258.

Gsaller F, Hortschansky P, Furukawa T, Carr PD, Rash B, Capilla J, Muller C, Bracher F, Bowyer P, Haas H, *et al.* (2016). Sterol Biosynthesis and Azole Tolerance Is Governed by the Opposing Actions of SrbA and the CCAAT Binding Complex. PLoS Pathog 12, e1005775.

Gutierrez-Correa M, Ludena Y, Ramage G, Villena GK (2012). Recent advances on filamentous fungal biofilms for industrial uses. Appl Biochem Biotechnol 167, 1235–1253.

Hamblin MR (2018). Mechanisms and Mitochondrial Redox Signaling in Photobiomodulation. Photochem Photobiol 94, 199–212.

Hernandez-Gonzalez M, Bravo-Plaza I, Pinar M, de Los Rios V, Arst HN Jr, Penalva MA (2018). Endocytic recycling via the TGN underlies the polarized hyphal mode of life. Plos Genet 14, e1007291.

Hoffmann S, Orlando M, Andrzejak E, Bruns C, Trimbuch T, Rosenmund C, Garner CC, Ackermann F (2019). Light-activated ROS production induces synaptic autophagy. J Neurosci 39, 2163–2183.

Hughes AL, Todd BL, Espenshade PJ (2005). SREBP pathway responds to sterols and functions as an oxygen sensor in fission yeast. Cell 120, 831–842.

Hung YH, Chen LM, Yang JY, Yang WY (2013). Spatiotemporally controlled induction of autophagy-mediated lysosome turnover. Nat Commun 4, 2111.

Hyde GJ, Davies D, Cole L, Ashford AE (2002). Regulators of GTP-binding proteins cause morphological changes in the vacuole system of the filamentous fungus, Pisolithus tinctorius. Cell Motil Cytoskeleton 51, 133–146.

Idnurm A (2013). Light sensing in Aspergillus fumigatus highlights the case for establishing new models for fungal photobiology. MBio 4, e00260–e00213.

Idnurm A, Verma S, Corrochano LM (2010). A glimpse into the basis of vision in the kingdom Mycota. Fungal Genet Biol 47, 881–892.

Jacobson K, Rajfur Z, Vitriol E, Hahn K (2008). Chromophore-assisted laser inactivation in cell biology. Trends Cell Biol 18, 443–450.

Jarvela TS, Linstedt AD (2014). The application of KillerRed for acute protein inactivation in living cells. Curr Protoc Cytom 69, 12 35 11-12 35 10.

Joyner RP, Tang JH, Helenius J, Dultz E, Brune C, Holt LJ, Huet S, Muller DJ, Weis K (2016). A glucose-starvation response regulates the diffusion of macromolecules. Elife (Cambridge) 5.

Kaur S, Singh S (2014). Biofilm formation by Aspergillus fumigatus. Med Mycol 52, 2–9.

Kershaw MJ, Talbot NJ (2009). Genome-wide functional analysis reveals that infection-associated fungal autophagy is necessary for rice blast disease. Proc Natl Acad Sci USA 106, 15967–15972.
Kessel D, Oleinick NL (2009). Initiation of autophagy by photodynamic therapy. Methods Enzymol 453, 1–16.
Klionsky DJ, Cregg JM, Dunn WA Jr, Emr SD, Sakai Y, Sandoval IV, Sibirny A, Subramani S, Thumm M, Veenhuis M, Ohsumi Y. (2003). A unified nomenclature for yeast autophagy-related genes. Dev Cell 5, 539–545.
Kowalski CH, Morelli KA, Schultz D, Nadell CD, Cramer RA (2020). Fungal biofilm architecture produces hypoxic microenvironments that drive antifungal resistance. Proc Natl Acad Sci USA 117, 22473–22483.
Lane N (2006). Cell biology: power games. Nature 443, 901–903.
Marini G, Nuske E, Leng W, Alberti S, Pigino G (2020). Reorganization of budding yeast cytoplasm upon energy depletion. Mol Biol Cell 31, 1232–1245.
Markina-Inarrairaegui A, Pantazopoulou A, Espeso EA, Penalva MA (2013). The Aspergillus nidulans peripheral ER: Disorganization by ER stress and persistence during mitosis. PLoS One 8, e67154.
Mazure NM, Pouyssegur J (2010). Hypoxia-induced autophagy: cell death or cell survival? Curr Opin Cell Biol 22, 177–180.
Munder MC, Midtvedt D, Franzmann T, Nuske E, Otto O, Herbig M, Ulbricht E, Muller P, Taubenberger A, Maharana S, *et al*. (2016). A pH-driven transition of the cytoplasm from a fluid- to a solid-like state promotes entry into dormancy. Elife (Cambridge) 5.
Mustafa AK, Gadalla MM, Sen N, Kim S, Mu W, Gazi SK, Barrow RK, Yang G, Wang R, Snyder SH (2009). H2S signals through protein S-sulfhydration. Sci Signal 2, ra72.
Nayak T, Szewczyk E, Oakley CE, Osmani A, Ukil L, Murray SL, Hynes MJ, Osmani SA, Oakley BR (2006). A versatile and efficient gene-targeting system for Aspergillus nidulans. Genetics 172, 1557–1566.
Osipov AN, Machneva TV, Buravlev EA, Vladimirov YA (2018). Effects of laser radiation on mitochondria and mitochondrial proteins subjected to nitric oxide. Front Med (Lausanne) 5, 112.
Pantazopoulou A (2016). The Golgi apparatus: insights from filamentous fungi. Mycologia 108, 603–622.
Pantazopoulou A, Penalva MA (2009). Organization and dynamics of the Aspergillus nidulans Golgi during apical extension and mitosis. Mol Biol Cell. 20, 4335–4347.
Pantazopoulou A, Pinar M, Xiang X, Penalva MA (2014). Maturation of late Golgi cisternae into RabE(RAB11) exocytic post-Golgi carriers visualized in vivo. Mol Biol Cell. 25, 2428–2443.
Park HS, Jun SC, Han KH, Hong SB, Yu JH (2017). Diversity, application, and synthetic biology of industrially important Aspergillus fungi. Adv Appl Microbiol 100, 161–202.
Parzych KR, Klionsky DJ (2014). An overview of autophagy: morphology, mechanism, and regulation. Antioxid Redox Signal 20, 460–473.
Petrovska I, Nuske E, Munder MC, Kulasegaran G, Malinovska L, Kroschwald S, Richter D, Fahmy K, Gibson K, Verbavatz JM, Alberti S. (2014). Filament formation by metabolic enzymes is a specific adaptation to an advanced state of cellular starvation. Elife (Cambridge).
Pinar M, Pantazopoulou A, Penalva MA (2013). Live-cell imaging of Aspergillus nidulans autophagy: RAB1 dependence, Golgi independence and ER involvement. Autophagy 9, 1024–1043.
Pires RH, Cataldi TR, Franceschini LM, Labate MV, Fusco-Almeida AM, Labate CA, Palma MS, Soares Mendes-Giannini MJ (2016). Metabolic profiles of planktonic and biofilm cells of Candida orthopsilosis. Future Microbiol 11, 1299–1313.
Pollack JK, Harris SD, Marten MR. (2009). Autophagy in filamentous fungi. Fungal Genet Biol 46, 1–8.
Pontecorvo G, Roper JA, Hemmons LM, Macdonald KD, Bufton AW (1953). The genetics of Aspergillus nidulans. Adv Genet 5, 141–238.
Ramage G, Rajendran R, Gutierrez-Correa M, Jones B, Williams C. (2011). Aspergillus biofilms: clinical and industrial significance. Fems Microbiol Lett 324, 89–97.
Ranftler C, Meisslitzer-Ruppitsch C, Neumuller J, Ellinger A, Pavelka M (2017). Golgi apparatus dis- and reorganizations studied with the aid of 2-deoxy-D-glucose and visualized by 3D-electron tomography. Histochem Cell Biol 147, 415–438.
Richie DL, Askew DS (2008). Autophagy in the filamentous fungus Aspergillus fumigatus. Methods Enzymol 451, 241–250.
Richie DL, Fuller KK, Fortwendel J, Miley MD, McCarthy JW, Feldmesser M, Rhodes JC, Askew DS (2007). Unexpected link between metal ion deficiency and autophagy in Aspergillus fumigatus. Eukaryotic Cell 6, 2437–2447.
Riquelme M, Aguirre J, Bartnicki-Garcia S, Braus GH, Feldbrugge M, Fleig U, Hansberg W, Herrera-Estrella A, Kamper J, Kuck U, *et al*. (2018). Fungal morphogenesis, from the polarized growth of hyphae to complex reproduction and infection structures. Microbiol Mol Biol Rev 82.
Rossanese OW, Soderholm J, Bevis BJ, Sears IB, O'Connor J, Williamson EK, Glick BS (1999). Golgi structure correlates with transitional endoplasmic reticulum organization in Pichia pastoris and Saccharomyces cerevisiae. J Cell Biol 145, 69–81.
Sano Y, Watanabe W, Matsunaga S (2014). Chromophore-assisted laser inactivation—towards a spatiotemporal-functional analysis of proteins, and the ablation of chromatin, organelle and cell function. J Cell Sci 127, 1621–1629.
Schellens JP, Vreeling-Sindelarova H, Plomp PJ, Meijer AJ (1988). Hepatic autophagy and intracellular ATP. A morphometric study. Exp Cell Res 177, 103–108.
Scherz-Shouval R, Elazar Z (2011). Regulation of autophagy by ROS: physiology and pathology. Trends Biochem Sci 36, 30–38.
Scherz-Shouval R, Shvets E, Fass E, Shorer H, Gil L, Elazar Z (2007). Reactive oxygen species are essential for autophagy and specifically regulate the activity of Atg4. EMBO J 26, 1749–1760.
Serrage H, Heiskanen V, Palin WM, Cooper PR, Milward MR, Hadis M, Hamblin MR (2019). Under the spotlight: mechanisms of photobiomodulation concentrating on blue and green light. Photochem Photobiol Sci 18, 1877–1909.
Shoji JY, Arioka M, Kitamoto K (2006a). Possible involvement of pleiomorphic vacuolar networks in nutrient recycling in filamentous fungi. Autophagy 2, 226–227.
Shoji JY, Arioka M, Kitamoto K (2006b). Vacuolar membrane dynamics in the filamentous fungus Aspergillus oryzae. Eukaryotic Cell 5, 411–421.
Shoji JY, Kikuma T, Arioka M, Kitamoto K (2010). Macroautophagy-mediated degradation of whole nuclei in the filamentous fungus Aspergillus oryzae. PLoS One 5, e15650.
Shukla N, Osmani AH, Osmani SA (2017). Microtubules are reversibly depolymerized in response to changing gaseous microenvironments within Aspergillus nidulans biofilms. Mol Biol Cell 28, 634–644.
Singh R, Cuervo AM (2011). Autophagy in the cellular energetic balance. Cell Metab 13, 495–504.
Suresh S, Markossian S, Osmani AH, Osmani SA (2017). Mitotic nuclear pore complex segregation involves Nup2 in Aspergillus nidulans. J Cell Biol 216, 2813–2826.
Takemoto K, Matsuda T, Sakai N, Fu D, Noda M, Uchiyama S, Kotera I, Arai Y, Horiuchi M, Fukui K, *et al*. (2013). SuperNova, a monomeric photosensitizing fluorescent protein for chromophore-assisted light inactivation. Sci Rep 3, 2629.
Tan Q, Wang M, Yu M, Zhang J, Bristow RG, Hill RP, Tannock IF (2016). Role of autophagy as a survival mechanism for hypoxic cells in tumors. Neoplasia 18, 347–355.
Trewin AJ, Berry BJ, Wei AY, Bahr LL, Foster TH, Wojtovich AP (2018). Light-induced oxidant production by fluorescent proteins. Free Radic Biol Med 128, 157–164.
Veses V, Richards A, Gow NA (2008). Vacuoles and fungal biology. Curr Opin Microbiol 11, 503–510.
Villena GK, Gutierrez-Correa M (2007). Morphological patterns of Aspergillus niger biofilms and pellets related to lignocellulolytic enzyme productivities. Lett Appl Microbiol 45, 231–237.
Voigt O, Poggeler S (2013). Self-eating to grow and kill: autophagy in filamentous ascomycetes. Appl Microbiol Biotechnol 97, 9277–9290.
Wang Y, Nartiss Y, Steipe B, McQuibban GA, Kim PK (2012). ROS-induced mitochondrial depolarization initiates PARK2/PARKIN-dependent mitochondrial degradation by autophagy. Autophagy 8, 1462–1476.
Wang M, Zhao J, Zhang L, Wei F, Lian Y, Wu Y, Gong Z, Zhang S, Zhou J, Cao K, *et al*. (2017). Role of tumor microenvironment in tumorigenesis. J Cancer 8, 761–773.
Willger SD, Puttikamonkul S, Kim KH, Burritt JB, Grahl N, Metzler LJ, Barbuch R, Bard M, Lawrence CB, Cramer RA Jr (2008). A sterol-regulatory element binding protein is required for cell polarity, hypoxia adaptation, azole drug resistance, and virulence in Aspergillus fumigatus. PLoS Pathog 4, e1000200.
Wojtovich AP, Foster TH (2014). Optogenetic control of ROS production. Redox Biol 2, 368–376.
Xie Z, Nair U, Klionsky DJ (2008). Atg8 controls phagophore expansion during autophagosome formation. Mol Biol Cell 19, 3290–3298.
Yanagisawa S, Kikuma T, Kitamoto K (2013). Functional analysis of Aoatg1 and detection of the Cvt pathway in Aspergillus oryzae. Fems Microbiol Lett 338, 168–176.

Yang L, Ukil L, Osmani A, Nahm F, Davies J, De Souza CP, Dou X, Perez-Balaguer A, Osmani SA (2004). Rapid production of gene replacement constructs and generation of a green fluorescent protein-tagged centromeric marker in Aspergillus nidulans. Eukaryotic cell 3, 1359–1362.

Yang JY, Yang WY. (2011). Spatiotemporally controlled initiation of Parkin-mediated mitophagy within single cells. Autophagy 7, 1230–1238.

Yoo H, Triandafillou C, Drummond DA (2019). Cellular sensing by phase separation: Using the process, not just the products. J Biol Chem 294, 7151–7159.

Yu Z, Fischer R (2019). Light sensing and responses in fungi. Nat Rev Microbiol 17, 25–36.

Zhu XM, Li L, Wu M, Liang S, Shi HB, Liu XH, Lin FC (2019). Current opinions on autophagy in pathogenicity of fungi. Virulence 10, 481–489.